Original Article

JOURNAL OF COMPOSITE MATERIALS

Journal of Composite Materials
0(0) 1–10

DOI: 10.1177/00219983211002237
journals.sagepub.com/home/jcm
SAGE

3D printing of spent coffee ground derived biochar reinforced epoxy composites

Ahmed Alhelal, Zaheeruddin Mohammed, Shaik Jeelani and Vijaya K Rangari

Abstract

Semi-crystalline carbon biochar is derived from spent coffee grounds (SCG) by a controlled pyrolysis process at high temperature/pressure conditions. Obtained biochar is characterized using XRD, SEM, and TEM techniques. Biochar particles are in the micrometer range with nanostructured morphologies. The SCG biochar thus produced is used as reinforcement in epoxy resin to 3 D print samples using the direct-write (DW) method with 1 and 3 wt. % loadings. Rheology results show that the addition of biochar makes resin viscous, enabling it to be stable soon after print; however, it could also lead to clogging of resin in printer head. The printed samples are characterized for chemical, thermal and mechanical properties using FTIR, TGA, DMA and flexure tests. Storage modulus improved with 1 wt. % biochar addition up to 27.5% and flexural modulus and strength increased up to 55.55% and 43.30% respectively. However, with higher loading of 3 wt. % both viscoelastic and flexural properties of 3D printed samples drastically reduced thus undermining the feasibility of 3D printing biochar reinforced epoxies at higher loadings.

Keywords

3D Printing, composites, sustainable carbon, mechanical properties, thermoset, microscopy

Highlights

- Sustainable carbon biochar was derived from spent coffee grounds using pyrolysis.
- Feasibility of 3d-printing epoxy resin reinforced with biochar was explored.
- Properties improved for low loading of 1 wt.%, but drastically reduced for 3 wt.%.
- Primary reason for reduced properties of samples with higher loading was non-feasibility in printing of biochar reinforced epoxy matrix.

Introduction

There is a huge demand for viable technologies that allow to rapidly manufacture parts of complex shapes and distinct performance requirements in areas like aerospace,[1,2] marine,[3] automotive,[4] architectural,[5] electronics,[6,7] medical devices,[8–10] and even consumer products.[11,12] Conventional processing technologies such as molding could incur a cost of up to $1 million associated with molds.[13] The cost-effectiveness of 3 D printing versus other manufacturing processes like molding, casting, and machining makes it an attractive alternative manufacturing process. 3 D printing, layer by layer, allows for better control over manufacturing quality as well as flexibility for manufacturing parts with different and complex geometries.[14] Polymers are considered the most common materials in **the** 3 D printing industry, mainly due to their variety and ease of handling for different 3 D printing processes. Polymers generally used for additive manufacturing are thermoplastic filaments, reactive monomers, resin, or powders. Although printing of thermoplastics is well established, the printing of thermosets is still a challenging task.[15,16]

Department of Materials Science and Engineering, Tuskegee University, USA

Corresponding author:
Vijaya K Rangari, Department of Materials Science and Engineering, Tuskegee University, 1200 West Montgomery Road, Tuskegee, AL 36088, USA.
Email: vrangari@tuskegee.edu

Unlike thermoplastic filaments which do not require polymerization[17,18] or photo/UV sensitive resins which instantly polymerize upon activation,[19,20] epoxy resins require reactive mechanisms that initially exhibit low viscosity which rises over time as the reaction proceeds under ambient conditions. These curing behaviors to maintain printed shape can be controlled by maintaining resin chemistry, temperature, and resin viscosity.[21] Even though thermosets have a competitive advantage over thermoplastics in terms of performance, their full potential can be realized only if they enter the fields of rapid manufacturing like 3 D printing. It is important to note that thermosets do experience shrinkage during curing that can lead to warping in geometrically complex parts.[22] However, shrinkage can be limited through the choice of curing agent and filler material, and preliminary experiments on large-scale Additive Manufacturing (AM) of thermoset polymers show significant promise.[23] Direct write (DW) 3 D printing is different from other additive manufacturing techniques. It does not require melting and extrusion of feed material through **the** print head, which is a norm in thermoplastic printing.[24] In **the** case of thermoset materials printed using DW process the curing starts after some time of deposition, which results in good interlayer bonding between the layers along build direction. Because of this, there is **a** drastic improvement in bond strength when compared to printed thermoplastics which generally have low strength in **the** build direction.[25–27] Successful printing of thermosets involves **the** introduction of different fillers such as nanoclay, graphene, Carbon Nanotubes, etc., or some modification of resin chemistry to produce a resin that can maintain form after coming out of the deposition nozzle.[23,24] The addition of filler can improve the rheology of epoxy and facilitate the printing process as well as enhance the mechanical properties of printed parts.[28]

Traditionally nanomaterials have been used for reinforcement of composites due to increased surface area and unique properties such as good thermal and electrical conductivity, enhanced fire retardancy, excellent strength to weight ratio.[29,30] There is significant potential for nanocomposite production through 3 D printing. Researchers have used nanoparticles to enhance tensile properties of the 3 D printed parts and have shown that with **the** addition of 5 wt.% nanotitanium dioxide (TiO_2),[31] 10 wt.% carbon-nanofiber[32] or 10 wt.% multi-walled carbon nanotube[33]showed a 13.2%, 39%, and 7.5% increase in the tensile strength of printed composite parts compared with unfilled polymer parts, respectively. Carbon-based materials have been recognized as excellent alternative fillers for manufacturing polymer composites with enhanced thermal stability, electrical, and tensile properties. However, the biggest obstacle **to** using such carbon-based material is their cost and dependence on fossil fuels. Researchers now are looking for carbon-based filler reinforcements, which can be generated from sustainable sources and can be produced in large quantities. In particular, waste biomasses are attracting much interest for the production of carbon filler called biochar.

Biochar is a carbon-rich product generated from thermochemical pyrolysis of biomass materials in an inert environment. Biochar was investigated for various applications such as soil remediation, catalysis, energy storage, and carbon capture.[34] It is considered that when biochar is reinforced with viscous epoxy matrix during fabrication, due to porous structure of biochar the epoxy can infiltrate to create mechanical interlocking by means of physical interactions. As a consequence, mechanical and thermal properties can be improved. Biochar derived from pine wood produced at 500 °C and activated at 900 °C was used as a filler material with polypropylene to improve mechanical properties.[35] Arrigo et.al reported that **polyethylene** reinforced with biochar derived from waste coffee grounds showed good thermal stability particularly improving the decomposition temperatures.[36] In another study PLA/PTT blend was reinforced with Miscanthus-based biochar, it was found that impact properties hugely depended on biochar particle size distribution. Biochar with a particle size range of 75−20 μm resulted in improved dispersion and improved energy dissipation. The resulting composite had an impact strength of 85 J/m, which is relatively high considering the brittle nature of the blend.[37] Recently Idrees et.al have used packaging waste-derived biochar as filler material for recycled PET composite using **a** 3 D printing technique. It was found that biochar reinforcement was able to improve **the** thermal, mechanical, and dynamic properties of the material.[38] Biochar as the filler has also been investigated with thermosets. Pine cone char and china poplar char, obtained after a 450 °C pyrolysis process, were used to produce biochar to fill epoxy resin at 10, 20, and 30 wt.%. It was found that general improvement of elastic properties of composites **was** obtained, china poplar char reported **the** best result compared with the pine cone char at **the** same loading percentages.[39] In another study Khan et al. investigated mechanical and microwave properties of epoxy composites reinforced with biochar derived from maple wood treated at 950 °C, it was found that biochar was effective in increasing mechanical and microwave properties with up to 20% loading.[40]

Even though there are separate studies are available for DW 3 D printing of epoxy composites and biochar reinforced epoxy composites, **there are no studies on**

feasibility of epoxy 3 D printing with biochar reinforcement. In this work, for the first time, we report **the** feasibility of 3 D printed biochar reinforced epoxy composites using **the** DW 3 D printing technique. A detailed study of spent coffee grounds (SPG) derived biochar from pyrolysis along with viscoelastic, thermal, and flexural properties of 3 D printed epoxy composites are reported.

Materials and methods

Materials

A diglycidyl ether of Bisphenol-A based 150 thick epoxy system (EPOTUF 37-140) with 1:1 epoxy hardner ratio was purchased from US Composites, West Palm Beach, Florida. Spent Coffee Ground (SCG) obtained from local McDonalds restaurant were used for biochar synthesis.

Biochar synthesis and dispersion

SCG were first washed and dried in an oven at 50 °C for two hours. Then, 20 g of SCG were burned in an autogenic high pressure/temperature reactor (GSL-1100X-RC). The chamber was purged with nitrogen for about 30 minutes to remove entrapped oxygen within the reactor. The SCG was then heated up to 800 °C at a rate of 20 °C/min and held at 800° C for 2 hours at autogenic pressure of about 150 bar. The resulting biochar was ground and sieved to be under 100 µm. Obtained biochar was dispersed into part A of epoxy system via ultrasonication method. Biochar was directly added to epoxy part A and sonicated for one hour at an amplitude of 60% and 20Sec On 30 Sec OFF pulse mode. The mixture of part A (infused with Biochar) and Hardener (part B) were then stirred for about 3 minutes using mechanical mixer at 2000 rpm followed by centrifugal mixing at 2000 rpm for 10 minutes. These compositions were fed into cartridge syringes using spatula and printed the samples using 3 D printing process as shown in Figure 1.

Printing procedure

The biochar reinforced epoxy mixture was fed to cartridge syringe which was fixed onto printer head drive system on a Hyrel-30M benchtop 3 D printer shown in Figure 2(a) from Hyrel, Atlanta, Georgia (USA). The syringe was driven by a printer head which provides necessary pressure for epoxy flow. The nozzle inner diameter was 0.19'', and printing speed was set to 50 mm/s. The CAD model of sample was made using FreeCAD software and sliced using Sli3r. The rectilinear infill type with 100% fill at 90° angle was used **to print the samples**.

The printer bed was maintained at different temperatures to accelerate curing process after material deposition. For the first layer bed was set at 60 °C and for each following layer an increment of 3° C was made to bed temperature to ensure partial curing to which the next layer can adhere, thus promoting interfacial adhesion between the layers. Each layer had a Z-axis increment of about 0.4 mm (thickness) and 14 such layers were printed on top of each other to achieve a rectangular plate like sample as shown in Figure 2(b). The samples were then removed from the printer bed and post cured in oven for another 2 hours at 100 °C. The thickness of all the final samples **(neat and biochar reinforced) was around 5.2 mm after curing.**

Characterization methods

The X-ray diffraction for carbon biochar was carried out using a Rigaku DMAX 2200 equipped with Cu cathode, Kα radiation with $\lambda = 1.54$ nm. Sample was scanned from 3° to 80° of 2θ angle at a rate of 2°/minute. Transmission electron microscope (TEM) analyses were carried out using JOEL JEM2010, 1 mg of biochar was dispersed in 5 mL ethanol using ultra sonication bath for 10 min. The colloidal solution was then deposited on copper grid for analysis. To study dispersion of biochar within epoxy and study fracture surfaces FE-SEM analysis was done using JEOL JSM 7200 F. The samples were cryo-fractured in liquid nitrogen and then coated with thin conductive layer of gold-palladium for 5 min. EDS analysis was also performed on carbon sample to look at elemental distribution.

To study the effects of viscosity on print parameters rheological studies were performed using TA Instruments AR-2000 rheometer equipped with 25 mm diameter ETC parallel plates with an initial gap of 600 µm. All measurements were preceded by a

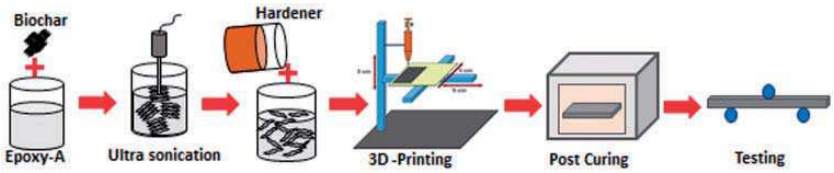

Figure 1. Schematic of 3D printed composite fabrication processes.

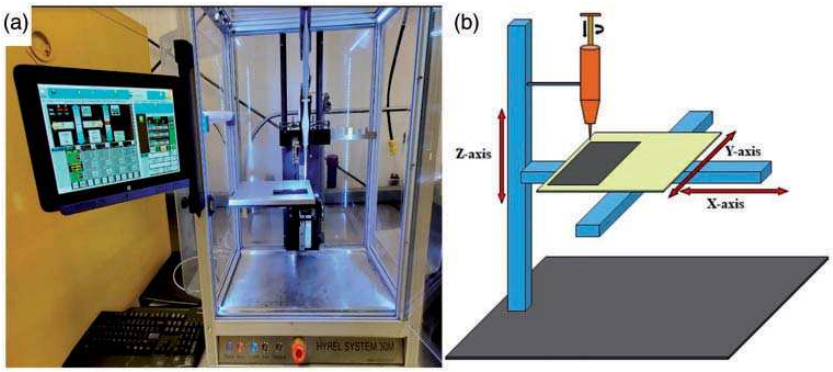

Figure 2. (a) 3D-printing setup. (b) Graphical representation of printing process.

1 min conditioning step at a constant shear rate of 0.1/s. **Steady state tests were performed by varying the shear rate from** 0.1 to 300 1/s at room temperature. Change in viscosity with respect to change in shear rate was recorded. Chemical analysis was performed by Fourier transform infrared-attenuated total reflectance (FTIR-ATR) (Thermo Scientific Nicolet iS5) using 32 averaged scans and 4 cm^{-1} resolutions over a range of 4000–400 cm^{-1}. Dynamic Mechanical Analysis (DMA) was done using non-isothermal mode of scans at 5 °C/min using TA Instruments Q800. The machine was purged with dry nitrogen at 50 mL/min. DSC scans were performed from 30 to 120 °C. Sample dimensions were 60 mm in length, 3-5 mm in thickness and 10-15 mm in width. Thermal stability and decomposition behavior was studied via thermogravimetric analysis (TGA) employing TA Instruments' Q-500. The equipment was purged with dry nitrogen at 90 and 10 mL/min for furnace and sample respectively. Samples were scanned from 30 to 750 °C at a ramp rate of 5 °C/min while data for sample weight loss was recorded as function of temperature.

Flexural strength and modulus was determined using three-point bending flexure test. Samples were prepared and tested according to ASTM 790 maintaining an L/d ratio of 16:1. Tests were conducted at room temperature and displacement mode using Zwick Roell testing machine with a load cell capacity 2.5 kN. Crosshead speed was 2.0 mm/min and the dimensions of sample were 3.5 mm in thickness, 12.5 mm in width and 80 mm in length. Flexural and DMA tests were conducted on samples along longitudinal print direction only.

Results and discussion

Figure 3 shows the X-ray diffractograms of coffee grounds derived biochar. It was found that there was formation of randomly arranged carbons structures. It is possible to prominently observe peaks around

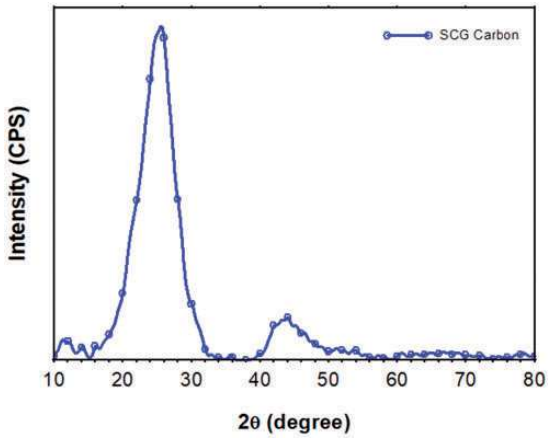

Figure 3. XRD pattern of spent coffee grounds derived biochar.

$2\theta = 24.5°$ and $2\theta = \mathbf{44}°$, corresponding to the diffraction of (002) and (100), respectively, which are graphite-like reflections. The high carbonization temperature combined with increased pressure results in an increased amount of fixed carbon and a higher graphitization degree; the organization of the carbon microstructure becomes well-ordered and condensed due to the elevated temperature. The highest peak at around 24° signifies an increasing regularity of crystalline structure, showing a tendency to result in a layer alignment. However, it can be noted that the carbon is not completely graphitized hence there are also some randomly arranged amorphous phases. Thus, it can be said that the carbon obtained is semi-crystalline.[41]

Figure 4(a) and (b) show the representative SEM micrographs of biochar produced from SCG at various maginifications. These images show that the particles are roughly spherical in shape with sizes combination of micrometer and nanomter range. The surface of the carbon has rough uneven morphologies with nanozize features as shown in Figure 4(b). Such morphologies can be useful in increasing the surface area of the biochar improving scope for biochar/matrix interactions

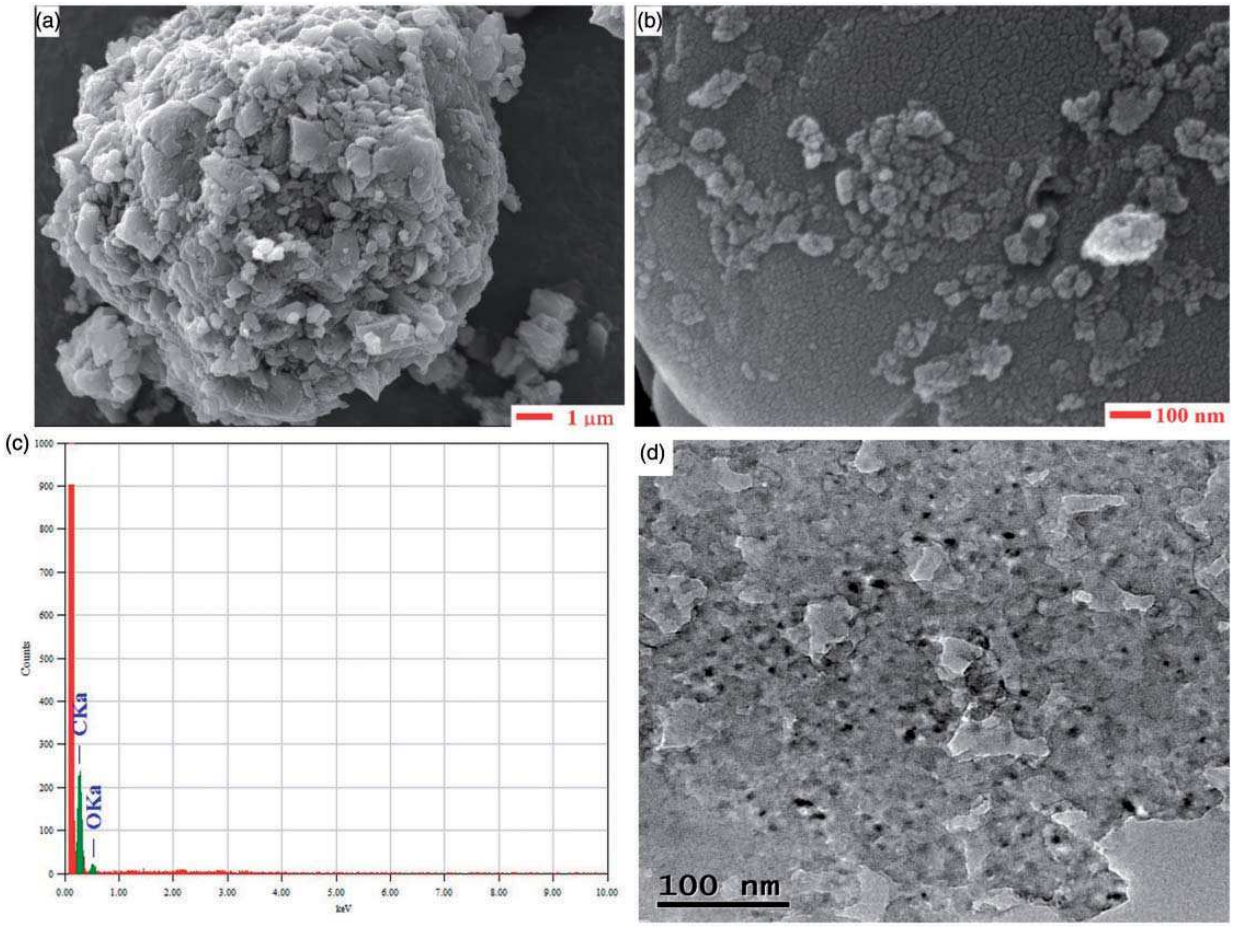

Figure 4. (a and b) SEM micrographs (c) EDS graph (d) TEM Micrograph of spent coffee grounds derived biochar.

for reinforcement applications. In Figure 4(c), the Energy Dispersive Spectroscopy (EDS) shows that the SCG has almost more than 95% carbon with trace amounts of oxygen and other elements. The TEM images clearly demonstrate carbon particles are semi-crystalline, with morphologies as small as 10 nm in size and spherical in shape, as shown in Figure 4(d). Such carbon particles with nanosize morphologies are very suitable for reinforcing fillers.[42]

FTIR spectra (Figure 5) shows that the broad band in the region 3317–3373 cm^{-1} corresponds to the stretching vibration of the hydroxyl groups (OH) of free and hydrogen bonded -OH groups. The peak at 1647 cm^{-1} is assigned to the (OH) bending vibration. The peaks at 2869 and 2921 cm^{-1} are attributed to C-H symmetric and asymmetric stretching vibration. The absorption peaks at 1607, 1582 and 1508 cm^{-1} are associated with characteristic adsorptions of the benzene ring of epoxy or C = C stretching of aromatic ring. The bands at 1362 and 1453 cm^{-1} can be attributed to CH3 and CH2 bending vibration, respectively. The C-O stretching of epoxide ring vibration showed peaks

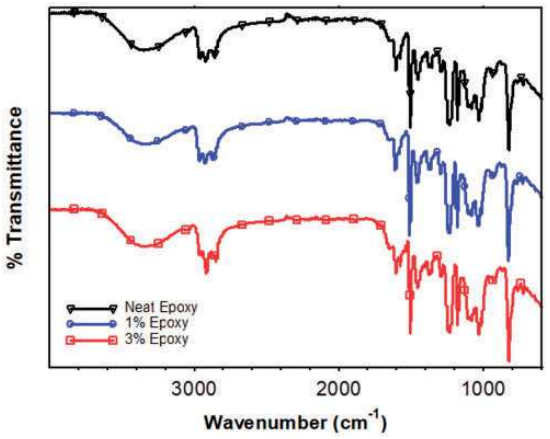

Figure 5. FTIR graphs of neat and biochar reinforced epoxy composites.

at 1237 and 917 cm^{-1}. The peak appeared at 826 cm-1 could be assigned to the 1,4-substitution of aromatic ring for epoxy resin. However, in case of 3% loaded epoxy peak corresponding to 2869 cm^{-1} were higher in

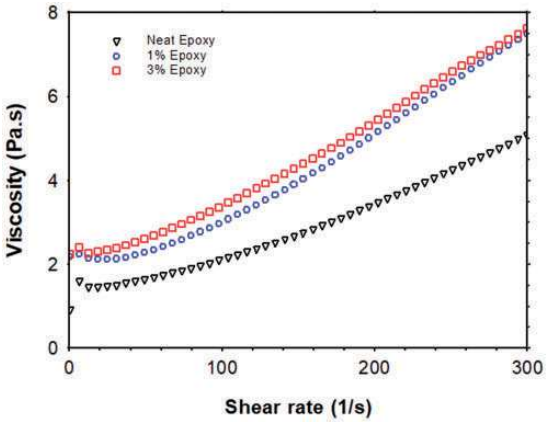

Figure 6. Rheology graphs of neat and biochar reinforced epoxy composites.

intensity due to presence of carbon from coffee grounds biochar which relates to symmetric stretching vibrations of C-H. It can be confirmed from the FTIR spectroscopy there were no signifificant changes peaks conforming that no strong covalent bonds were formed between the biochar and epoxy matrix confirming that the interactions were mostly due to hydrophobic **van der waals forces.**[43]

Rheological tests conducted on the uncured neat epoxy system and biochar reinforced epoxy system revealed that the viscosity increased with increasing time and shear rate in all the resin systems following a similar trend as shown in Figure 6. The reason for such behavior could be due to crosslinking and gelation of epoxy system with time. However, in case of biochar reinforced epoxy systems, the viscosity was higher at lower shear rates itself and increased dramatically with increasing shear rates which is common for micrometric filler reinforcement. This could happen due to either biochar/epoxy interactions or biochar/biochar interaction. This confirms the value of adding biochar to the epoxy system making it stable soon after printing, minimizing its chances of flowing away. However, it also leads to other issues like clogging of nozzle, resisted flow of polymer, which eventually could lead to improper printing of epoxy system especially for higher loadings.[36]

TGA analysis of neat epoxy resin compared to 1 wt. % and 3 wt. % biochar reinforced epoxy is shown in Figure 7. Onset of degradation i.e. (5% weight loss) was recorded at 325 °C for neat epoxy and was almost same for 1 wt. % biochar loaded epoxy, but for 3 wt. % samples it was around 328 °C. Rate of Maximum decomposition values derived from derivative weight change graphs were 365.47 °C for neat epoxy with a weight loos of 46% and 365.86 °C with weight loss of 46% and 366.96 °C with weight loss of 49% for 1 wt. % and 3 wt. % loaded samples respectively. Even though there was enough carbon loading, overall thermal properties did not improve very drastically showing negligible effects on thermal stability. Residue of the epoxy systems was higher for biochar-loaded epoxy composites due to presence of carbon, which is inherently more stable. Table 1 further gives the values corresponding to the rate of max decomposition, onset of degradation, and residue percentage as shown in Figure 7.[44]

The results from DMA graphs shown in Figure 8 illustrate storage modulus versus temperature of neat epoxy resin compared with biochar infused epoxy resin. The peak of the storage modulus curve is of interest to highlight the initial stiffness of the material at room temperature. It can be observed that the storage modulus was highest for 1 wt. % biochar loaded samples which was an improvement of about 27.5%. However, in case of 3 wt. % loaded samples storage modulus was drastically low with a reduction of about 21%. The modulus here is expected to be higher at least at room temperature but the reason for reduction could be improper printing of samples due to clogging of printer head resulting in poor cross linking of epoxy system or poor interfacial bonding among layers due to heavy loading. The peak of the tan delta curve, which indicates the glass transition temperature have revealed that with biochar loading Tg values were not very much affected. The modulus decreased for all samples with increase in temperature, the rate of modulus reduction was drastic in 1% loaded samples between 45–65°C, this drastic reduction could be due improper interface between biochar and polymer chains. Even though higher reinforcement loading is known for increasing modulus of the material, it is not very effective in 3 D printed parts using DW method.[38]

Flexural tests shown in Figure 9 revealed that the 3 D printing of epoxy resin had parts with acceptable mechanical properties. Hence making it a viable route for parts manufacturing. Neat epoxy samples had modulus of about 2.61 GPa. Upon addition of biochar at 1%, loading modulus improved for about 55% to 4.06 GPa. However, in case of 3% loading modulus drastically reduced to 1.42 GPa which is a reduction of about 46% shown in Table 2. This reduction in modulus of the samples suggests that at heavy loading percentages DW printing of epoxy could be challenging to maintain good interlayer bonding as well as hampering the cross linking of polymer chains. Similar results were obtained for strength values. Flexural strength (Figure 10(b)) of neat samples was around 87.8 MPa, which increase up to 125.82 MPa that is an improvement of 43% where as in case of 3 wt. % loading strength decreased 32% to a value of around 59 MPa

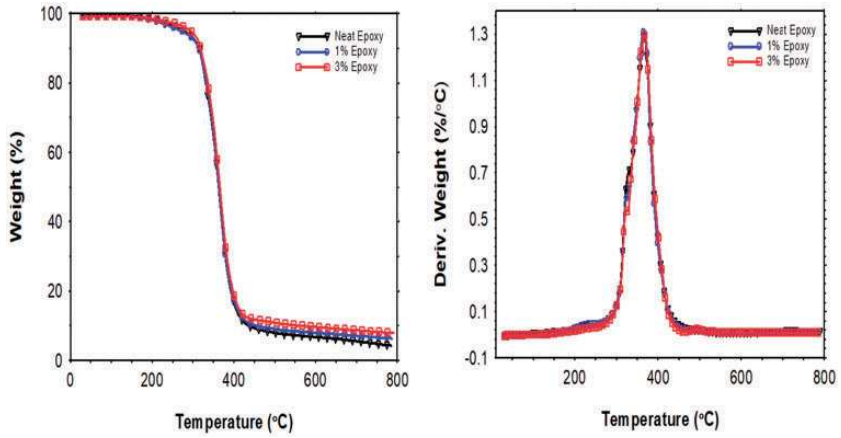

Figure 7. TGA graphs of neat and biochar reinforced epoxy composites.

Table 1. DMA and TGA results of neat and biochar-reinforced epoxy resin.

Sample	Glass transition tan delta (°C)	Storage modulus (MPa)	Rate of max decomposition (°C)	Onset of degradation (°C)	Residue %
Neat Epoxy	65.32	2131	365.47	325.01	4.34
1wt.% Epoxy	63.29	2716	365.86	326.30	7.31
3wt.% Epoxy	66.36	1687	366.96	328.22	8.64

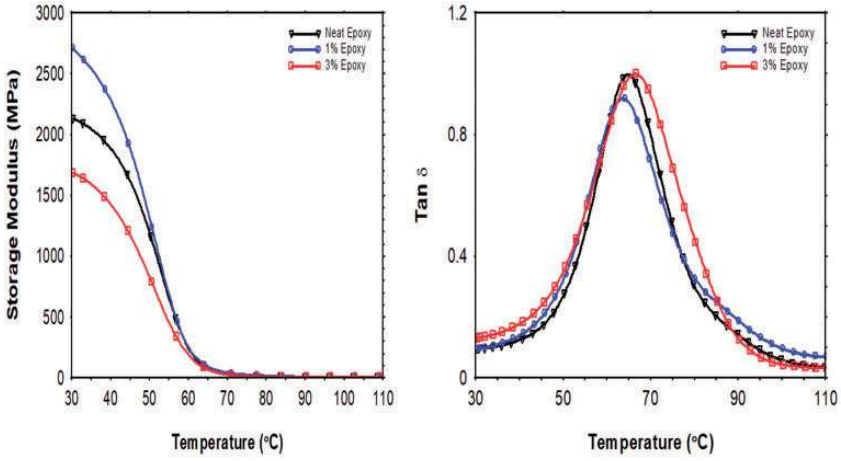

Figure 8. DMA graphs of neat and biochar reinforced epoxy composites.

thus undermine the feasibility of printing epoxy systems at higher reinforcement loading. In both the cases of 1 and 3% loading, **strain** values increased which is mainly due to improvement of ductility due to biochar reinforcement.[23]

SEM micrographs of neat 3 D printed part has shown good interface between different layers as shown in Figure 11(a). Thus, it can be inferred that DW method of 3 D printing can be useful in developing parts made of epoxy material. For SCG carbon reinforced epoxy samples it was found that for 1% loaded samples there was good dispersion of biochar carbon within epoxy (Figure 11(b)) whereas for 3% loading agglomeration of biochar was evident as shown in Figure 11(c). These agglomerations could lead low quality printing of samples and act as stress

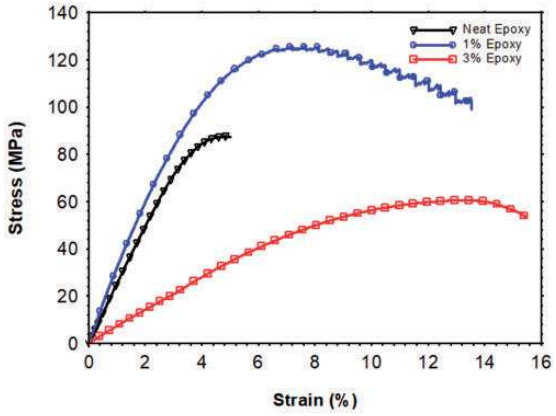

Figure 9. Flexural graph of neat and biochar reinforced epoxy composites.

concentration sites under loading leading to premature failure of samples, which was observed in DMA and flexure results.

Conclusions

In this study carbon- biochar is derived from a sustainable source of spent coffee grounds using high temperature/pressure reaction. Obtained biochar was semi-crystalline in nature due to high temperature and pressure, thus making it a potential reinforcement filler. Attempts were made to develop a simple 3 D printing method to fabricate biochar reinforced composite samples. Feasibility of biochar reinforced epoxy resin sample fabrication using Direct Write 3 D printing method was explored. Samples with good interfacial bonding among print layers were achieved. It was found that biochar reinforcement at lower loading of

Table 2. Flexural properties of neat and biochar-reinforced epoxy resin.

Sample	Flexural modulus (GPa)	% Change	Flexural strength (MPa)	% Change
Neat Epoxy	2.61 ± 0.08	–	87.8 ± 0.28	–
1wt.% Epoxy	4.06 ± 0.42	55.55	125.82 ± 4.41	43.30
3wt.% Epoxy	1.42 ± 0.13	−45.59	59.73 ± 4.63	−31.97

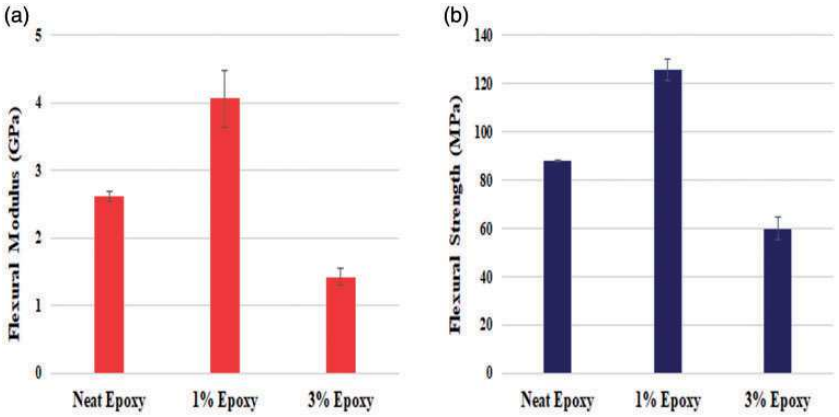

Figure 10. (a) Flexural modulus. (b) Flexural strength of neat and biochar reinforced epoxy composites.

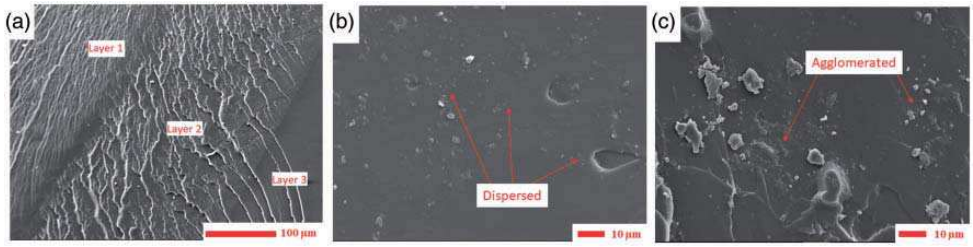

Figure 11. SEM micrographs of 3D printed (a) Neat epoxy (b) 1 wt. % (c) 3 wt. % biochar reinforced epoxy.

1 wt. % improved the mechanical properties of material. Storage modulus improved upto 27.5%, and flexural modulus and strength increased upto 55.55% and 43.30% respectively. However, with higher loading of 3 wt. % both storage modulus and flexural modulus decreased drastically, primary reason for such behavior was due to formation agglomerations and also improper crosslinking of polymer chains due to presence of high biochar content, thus undermining ability of printing biocahr reinforced epoxy composites at higher loading. To overcome this problem, if resin formulations which are less vicious for printability and easily curable soon after print without scope for agglomerations can be developed biochar reinforced epoxy parts can be developed using direct write 3 D printing method.

Declaration of Conflicting Interests

The author(s) declared no potential conflicts of interest with respect to the research, authorship, and/or publication of this article.

Funding

The author(s) disclosed receipt of the following financial support for the research, authorship, and/or publication of this article: The authors would like to acknowledge the financial support of funding agencies, Saudi Arabian Cultural Mission (SACM) and National Science Foundation's, NSF-MRI #1531934, NSF-AL-EPSCoR# 1655280, NSF CREST#1735971 and GRSP EPSCoR.

ORCID iDs

Zaheeruddin Mohammed https://orcid.org/0000-0001-5639-537X
Vijaya K Rangari https://orcid.org/0000-0002-3962-1686

References

1. Najmon JC, Raeisi S and Tovar A. Review of additive manufacturing technologies and applications in the aerospace industry. *Addit Manuf Aerosp Ind*. Epub ahead of print 1 January 2019. DOI: 10.1016/B978-0-12-814062-8.00002-9.
2. Hehr A, Wenning J, Norfolk M, et al. Selective reinforcement of aerospace structures using ultrasonic additive manufacturing. *J Mater Eng Perform* 2019; 28: 633–640.
3. Mohammed JS. Applications of 3D printing technologies in oceanography. *Methods Oceanogr* 2016; 17: 97–117.
4. Böckin D and Tillman A-M. Environmental assessment of additive manufacturing in the automotive industry. *J Clean Prod* 2019; 226: 977–987.
5. Wu P, Wang J and Wang X. A critical review of the use of 3-D printing in the construction industry. *Autom Constr* 2016; 68: 21–31.
6. Zhang F, Wei M, Viswanathan VV, et al. 3D printing technologies for electrochemical energy storage. *Nano Energy* 2017; 40: 418–431.
7. Valentine AD, Busbee TA, Boley JW, et al. Hybrid 3D printing of soft electronics. *Adv Mater* 2017; 29: 1703817.
8. Tappa K and Jammalamadaka U. Novel biomaterials used in medical 3D printing techniques. *J Funct Biomater* 2018; 9: 17.
9. Tack P, Victor J, Gemmel P, et al. 3D-printing techniques in a medical setting: a systematic literature review. *Biomed Eng Online* 2016; 15: 115.
10. Culmone C, Smit G and Breedveld P. Additive manufacturing of medical instruments: a state-of-the-art review. *Addit Manuf* 2019; 27: 461–473.
11. Bogers M, Hadar R and Bilberg A. Additive manufacturing for consumer-centric business models: Implications for supply chains in consumer goods manufacturing. *Technol Forecast Soc Change* 2016; 102: 225–239.
12. Park SJ, Lee JE, Lee HB, et al. 3D printing of bio-based polycarbonate and its potential applications in eco-friendly indoor manufacturing. *Addit Manuf* 2020; 31: 100974.
13. How to save time, reduce costs, and improve the quality of injection-molded parts with mold-filling simulation, www.solidworks.com/sw/docs/Plastics_MoldInjection_WP_FINAL_7.13.16.pdf. (2014, accessed 26 February 2021).
14. Gundrati NB, Chakraborty P, Zhou C, et al. First observation of the effect of the layer printing sequence on the molecular structure of three-dimensionally printed polymer, as shown by in-plane capacitance measurement. *Compos Part B: Eng* 2018; 140: 78–82.
15. Ladd C, So J-H, Muth J, et al. 3D printing of free standing liquid metal microstructures. *Adv Mater* 2013; 25: 5081–5085.
16. Mohammed Z, Jeelani S and Rangari V. Effect of low-temperature plasma treatment on surface modification of polycaprolactone pellets and thermal properties of extruded filaments. *JOM* 2020; 72: 1523–1532.
17. Yao T, Deng Z, Zhang K, et al. A method to predict the ultimate tensile strength of 3D printing polylactic acid (PLA) materials with different printing orientations. *Compos Part B: Eng* 2019; 163: 393–402.
18. Weng Z, Wang J, Senthil T, et al. Mechanical and thermal properties of ABS/montmorillonite nanocomposites for fused deposition modeling 3D printing. *Mater Des* 2016; 102: 276–283.
19. Voet VSD, Strating T, Schnelting GHM, et al. Biobased acrylate photocurable resin formulation for stereolithography 3D printing. *ACS Omega* 2018; 3: 1403–1408.
20. Bertana V, Pasquale GD, Ferrero S, et al. 3D printing with the commercial UV-Curable standard blend resin: optimized process parameters towards the fabrication of tiny functional parts. *Polymers* 2019; 11: 292.
21. Compton BG and Lewis JA. 3D-Printing of lightweight cellular composites. *Adv Mater* 2014; 26: 5930–5935.
22. Li C and Strachan A. Free volume evolution in the process of epoxy curing and its effect on mechanical properties. *Polymer* 2016; 97: 456–464.

23. Hmeidat NS, Kemp JW and Compton BG. High-strength epoxy nanocomposites for 3D printing. *Compos Sci Technol* 2018; 160: 9–20.
24. Compton BG, Hmeidat NS, Pack RC, et al. Electrical and mechanical properties of 3D-printed graphene-reinforced epoxy. *Jom* 2018; 70: 292–297.
25. Ahn SH, Montero M, Odell D, et al. Anisotropic material properties of fused deposition modeling ABS. *Rapid Prototyp J* 2002; 8: 248–257.
26. Duty CE, Kunc V, Compton B, et al. Structure and mechanical behavior of big area additive manufacturing (BAAM) materials. *Rapid Prototyp J* 2017; 23: 181–189.
27. Kishore V, Ajinjeru C, Nycz A, et al. Infrared preheating to improve interlayer strength of big area additive manufacturing (BAAM) components. *Addit Manuf* 2017; 14: 7–12.
28. Pleşa I, Noţingher P, Schlögl S, et al. Properties of polymer composites used in high-voltage applications. *Polymers* 2016; 8: 173.
29. Nguyen Q, Ngo T, Tran P, et al. Fire performance of prefabricated modular units using organoclay/glass fibre reinforced polymer composite. *Constr Build Mater* 2016; 129: 204–215.
30. Song J, Chen C and Zhang Y. High thermal conductivity and stretchability of layer-by-layer assembled silicone rubber/graphene nanosheets multilayered films. *Compos Part A: Appl Sci Manuf* 2018; 105: 1–8.
31. Chung H and Das S. Processing and properties of glass bead particulate-filled functionally graded nylon-11 composites produced by selective laser sintering. *Mater Sci Eng A* 2006; 437: 226–234.
32. Shofner ML, Lozano K, Rodríguez-Macías FJ, et al. Nanofiber-reinforced polymers prepared by fused deposition modeling. *J Appl Polym Sci* 2003; 89: 3081–3090.
33. Sandoval JH and Wicker RB. Functionalizing stereolithography resins: effects of dispersed multi-walled carbon nanotubes on physical properties. *Rapid Prototyp J* 2006; 12: 292–303.
34. Zheng W, Guo M, Chow T, et al. Sorption properties of greenwaste biochar for two triazine pesticides. *J Hazardous Mater* 2010; 181: 121–126.
35. Ikram S, Das O and Bhattacharyya D. A parametric study of mechanical and flammability properties of biochar reinforced polypropylene composites. *Compos Part A: Appl Sci Manuf* 2016; 91: 177–188.
36. Arrigo J, Jagdale P, Bartoli T, et al. Structure–property relationships in polyethylene-based composites filled with biochar derived from waste coffee grounds. *Polymers* 2019; 11: 1336.
37. Nagarajan V, Mohanty AK and Misra M. Biocomposites with size-fractionated biocarbon: influence of the microstructure on macroscopic properties. *ACS Omega* 2016; 1: 636–647.
38. Idrees M, Jeelani S and Rangari V. Three-dimensional-printed sustainable biochar-recycled PET composites. *ACS Sustainable Chem Eng* 2018; 6: 13940–13948.
39. Oral I. Determination of elastic constants of epoxy resin/biochar composites by ultrasonic pulse echo overlap method. *Polym Compos* 2016; 37: 2907–2915.
40. Khan A, Savi P, Quaranta S, et al. Low-cost carbon fillers to improve mechanical properties and conductivity of epoxy composites. *Polymers* 2017; 9: 642.
41. Alves AC, Antero RV, Oliveira SB, et al. Activated carbon produced from waste coffee grounds for an effective removal of bisphenol-A in aqueous medium. *Environ Sci Pollut Res* 2019; 26: 24850–24862.
42. Das O, Sarmah AK and Bhattacharyya D. A sustainable and resilient approach through biochar addition in wood polymer composites. *Sci Total Environ* 2015; 512–513: 326–336.
43. Loos MR, Coelho LA, Pezzin SH, et al. Effect of carbon nanotubes addition on the mechanical and thermal properties of epoxy matrices. *Mat Res* 2008; 11: 347–352.
44. Bartoli M, Rosso C, Giorcelli M, et al. Effect of incorporation of microstructured carbonized cellulose on surface and mechanical properties of epoxy composites. *J Appl Polym Sci* 2020; 137: 48896.